Systems & Control Letters 161 (2022) 105131

Contents lists available at ScienceDirect

Systems & Control Letters

journal homepage: www.elsevier.com/locate/sysconle

Event-triggered control for linear time-varying systems using a positive systems approach☆

Frederic Mazenc [a,1], Michael Malisoff [b,*,1], Corina Barbalata [c,1], Zhong-Ping Jiang [d,1]

[a] Inria Saclay, L2S-CNRS-CentraleSupélec, 3 rue Joliot Curie, 91192, Gif-sur-Yvette, France
[b] Department of Mathematics, Louisiana State University, Baton Rouge, LA 70803-4918, USA
[c] Department of Mechanical and Industrial Engineering, Louisiana State University, Baton Rouge, LA 70803, USA
[d] Department of Electrical and Computer Engineering, New York University, Brooklyn, NY 11201, USA

ARTICLE INFO

Article history:
Received 8 June 2021
Received in revised form 26 October 2021
Accepted 3 January 2022
Available online 7 February 2022

Keywords:
Stability
Event-triggered
Observer
Positive systems

ABSTRACT

This paper presents a new design for the event-triggered output feedback control of uncertain linear time-varying systems. Departing from the traditional treatments of event-triggered linear time-invariant systems, it is shown that factoring of fundamental solutions as products of solutions of matrix differential equations, together with small-gain arguments and the notions of interval observers and positive systems, lead to a new class of robust event-triggered output-feedback controllers. A key innovation is our use of new event triggers, which use vectors of absolute values instead of the usual Euclidean 2-norms. An illustrative example of a curve tracking system from marine robotics validates the efficacy of the proposed design scheme.

1. Introduction

Event-triggered control plays a significant role in current controls research; see, e.g., the works [1–8], and [9]. An advantage of event-triggered control is its ability to reduce the computational burden associated with control implementations, by only changing control values when a significant event occurs. Such events are usually characterized as times when the state of the system enters a prescribed region. This differs from standard zero-order hold control strategies, which instead usually recompute the control values at times that are independent of the state. As shown in [10], event-triggered control is fundamentally a control problem for an interconnection consisting of the controlled plant and the event-triggering mechanism. Several previous event-triggered control design schemes can be unified from a small-gain perspective [11].

Emerging computing methods may facilitate recomputing control values. However, the increasing use of shared wired (or shared wireless) networked control systems strongly motivates designing controls that can take communication, computation, and energy constraints into account [3]. This has led to multiple event-triggered control designs, such as those in [8,9,12], and [13]. A different body of current control theoretic research is based on positive systems, meaning, systems for which the nonnegative orthant is a positively invariant set. This has led to new control analysis and designs that help overcome the challenges of applying traditional Lyapunov function approaches. Several works on positive systems are based on interval observers (as defined, e.g., in [14–16]), which yield intervals containing values of estimated states at each time, where the inequalities involving vector valued functions are viewed componentwise; see [17] and Section 2. Interval observers and positive systems led to advances in aerospace engineering, mathematical biology, and other applications.

This (and the need to consider linear time-varying systems with uncertain coefficients and output feedback in applications) motivates this work. Here, we develop a new event-triggered control technique based on the theory of positive systems. The positive system will be the dynamics for $(\overline{x}, -\underline{x})$, where $(\underline{x}, \overline{x})$ is the state of an interval observer (for an estimator $\hat{x}$ of unmeasured states). See (26), where $\underline{x}$ is then multiplied by -1 to obtain a dynamics for $(\overline{x}, -\underline{x})$ that is a positive system, which is essential for proving the exponential stability of our event-triggered system. We believe that our work is the first to apply positive systems and interval observer methods to event-triggered output feedback control for systems with uncertain dynamics.

☆ Supported by NSF, USA Grants 2009659 (Malisoff and Barbalata) and 2009644 (Jiang). A preliminary version was accepted for the 2021 European Control Conference; see Section 1 for a comparison between this work and the conference version.

* Corresponding author.
E-mail addresses: frederic.mazenc@l2s.centralesupelec.fr (F. Mazenc), malisoff@lsu.edu (M. Malisoff), cbarbalata@lsu.edu (C. Barbalata), zjiang@nyu.edu (Z.-P. Jiang).

[1] The authors collaborated on all parts of the paper.

https://doi.org/10.1016/j.sysconle.2022.105131
0167-6911/

Our global exponential stability proof uses interval observers as comparison systems, and the linear Lyapunov function approach from works such as [17], [18], and [19, Chapt. 3]. However, [17] does not cover event-triggering. Significant innovations in our work include (1) our covering time-varying systems, using new methods that are beyond the scope of traditional treatments of event-triggered linear time-invariant systems, such as our factoring of fundamental solutions as products of solutions of matrix differential equations, (2) our novel approaches to finding lower bounds on the times between event triggering times, and (3) our new theorem that ensures global exponential stability even when there is uncertainty in the dynamics, which uses our novel small-gain approach to output feedback control. Other significant innovations in our work include (4) our use of matrices of absolute values instead of the usual matrix 2-norm, which, in our examples, leads to larger lower bounds on the inter-sample times between the event-triggering times and therefore provides an advantage compared with existing event-triggered controls, and (5) the integration of small-gain arguments and positive system theory for tackling the event-triggered control of linear time-varying systems with output feedback and uncertainty in the system matrices. Our use of matrices of absolute values instead of standard Euclidean 2-norms is a key innovation that makes it possible to use our positive systems and interval observer methods.

We review our definitions and notation in Section 2. We introduce our class of time-varying systems and our assumptions in Section 3. In Section 4, we present our event-triggered control design, and we state our theorem on the asymptotic convergence properties that our closed-loop systems enjoy when using this control design. In Section 5, we prove our theorem. In Section 6, we illustrate our method in a marine robotic dynamics and other cases. We end in Section 7 with our suggestions for future research.

In addition to addressing the essential difficulties of achieving event-triggered control for linear systems with outputs and uncertain coefficient matrices, this paper improves on our conference version [20]. The improvements are our covering time-varying systems (which call for using fundamental solutions instead of matrix exponentials), and a proof of our theorem and a new application to a marine robotic system. These three features were not present in [20], which was confined to time-invariant systems and which only provided sketches of proofs of theorems. Also, by including time-varying and uncertain coefficients and output feedback control, the theorem in this work includes the dynamics from all three theorems of [20], as special cases.

2. Definitions and notation

We use these definitions and this notation, where the dimensions of our Euclidean spaces are arbitrary unless we otherwise indicate. The arguments of functions are omitted when no confusion can arise from the context. Set $\mathbb{Z}_0 = \{0, 1, 2, \ldots\}$ and $\mathbb{N} = \mathbb{Z}_0 \backslash \{0\}$. Given a matrix $G = [g_{ij}] \in \mathbb{R}^{r\times s}$, we set $|G| = [|g_{ij}|]$, i.e., the entries of $|G|$ are the absolute values of the corresponding entries of G. We also set $G^+ = [\max\{g_{ij}, 0\}]$ and $G^- = G^+ - G$, and $\sup_{\ell\in J} |G(\ell)| = [m_{ij}]$ where $m_{ij} = \sup_{\ell\in J} |g_{ij}(\ell)|$ when G is a time-varying and bounded matrix-valued function and J is a subset of the domain of G. A square matrix is called Metzler provided all of its off-diagonal entries are nonnegative. We use inequalities of matrices, in the following entry-wise sense. Given two matrices $D = [d_{ij}]$ and $E = [e_{ij}]$ of the same size, we write $D < E$ (resp., $D \le E$) provided $d_{ij} < e_{ij}$ (resp., $d_{ij} \le e_{ij}$) for all i and j. We use similar notation for vectors. Hence, $|x| \in \mathbb{R}^n$ is a vector of absolute values of any vector $x \in \mathbb{R}^n$. A matrix M is called positive provided $M > 0$, where 0 is the zero matrix.

For a matrix $M = [m_{ij}]$ in $\mathbb{R}^{n\times n}$, we let D_M denote the diagonal matrix $\mathrm{diag}\{m_{11}, m_{22}, \ldots, m_{nn}\}$ in $\mathbb{R}^{n\times n}$. Hence, all of the main diagonal entries of $M - D_M$ are equal to zero. We let $R_M = D_M + (M - D_M)^+$ and $N_M = (M - D_M)^-$, so $M = R_M - N_M$. We let $\|\cdot\|$ denote the standard Euclidean norm of matrices and vectors, and we let $\|\cdot\|_\infty$ (resp., $\|\cdot\|_J$) denote the sup norm of matrix-valued functions in this norm over their domain (resp., an interval J in their domain). We let I be the identity matrix in any dimension, and we use the usual definition and properties of fundamental matrices, e.g., from [21, Appendix C]. We use $\Phi_{\mathcal{M}}$ to denote the fundamental matrix for a system of differential equations of the form $\dot z = \mathcal{M}(t)z$. We also use the standard definitions (e.g., from [10]) of class $\mathcal{KL}$ and $\mathcal{K}_\infty$ functions.

3. Class of systems and assumptions

We consider the system with an output y given by

$$\begin{cases} \dot x(t) = (A_0(t) + A_\delta(t))x(t) + (B_0(t) + B_\delta(t))u(t) \\ y(t) = Cx(t) \end{cases} \tag{1}$$

with x valued in $\mathbb{R}^n$, y valued in $\mathbb{R}^q$, the control u valued in $\mathbb{R}^p$, known bounded continuous matrix-valued functions A_0 and B_0, matrix-valued functions A_δ and B_δ whose entries are piecewise continuous and that can represent uncertainties, and a known constant matrix $C \in \mathbb{R}^{q\times n}$. In some of what follows, we set $A(t) = A_0(t)+A_\delta(t)$ and $B(t) = B_0(t)+B_\delta(t)$. Our main assumptions are as follows:

Assumption 1. There is a known bounded continuous matrix-valued function $L : \mathbb{R} \to \mathbb{R}^{n\times q}$ such that the system

$$\dot z(t) = \big(A(t) + L(t)C\big)z(t) \tag{2}$$

is uniformly globally exponentially stable to the origin on $\mathbb{R}^n$. Also, there are known constants $a_* \ge 0$ and $b_* \ge 0$ such that $\|A_\delta\|_\infty \le a_*$ and $\|B_\delta\|_\infty \le b_*$. □

Assumption 2. There are a matrix $\Gamma > 0$, a bounded continuous matrix-valued function $K : \mathbb{R} \to \mathbb{R}^{p\times n}$, a constant $p \ge 0$, a function $V : [0, +\infty) \to \mathbb{R}^n$ of class C^1, and two vectors $\overline{V} > 0$ and $\underline{V} > 0$ in $\mathbb{R}^n$ such that, with the choices

$$H(t) = A_0(t)+B_0(t)K(t) \text{ and } E(t) = R_H(t)+N_H(t), \tag{3}$$

we have

$$\underline{V} \le V(t) \le \overline{V} \tag{4}$$

and

$$\dot V(t)^\top + V(t)^\top\big(E(t) + |B_0(t)K(t)|\Gamma\big) \le -pV(t)^\top \tag{5}$$

for all $t \ge 0$. □

The motivation for Assumptions 1–2 is as follows. Assumption 1 is a time-varying analog of the usual requirements from the constant coefficient unperturbed case that (A, C) is observable, which is then robustified by including $A_\delta(t)$ in the coefficient matrix in (2). Hence, the required exponential stability condition for (2) will be satisfied if the unperturbed system $\dot z(t) = (A_0(t) + L(t)C)z(t)$ is uniformly globally exponentially stable to the origin on $\mathbb{R}^n$ when the sup norm of A_δ is small enough. Assumption 2 is a time-varying robustified analog of the usual requirement in the time-invariant case that H is Metzler and Hurwitz, in which case $H = R_H = E$; see [20] for our study of time-invariant cases, and [19, Lemma 2.3, p.41] for a proof that there are a positive constant vector $V \in \mathbb{R}^n$ and a constant $p > 0$ such that $V^\top H \le -pV^\top$ when $H \in \mathbb{R}^{n\times n}$ is a constant Metzler Hurwitz matrix.

Our rationale for calling Assumption 2 a robustified version of the preceding condition from [19] is that if there exist a positive vector $V \in \mathbb{R}^n$ and a positive scalar p such that $V^\top H(t) \leq -2pV^\top$ holds for all $t \geq 0$, and if $H(t)$ is Metzler for all $t \geq 0$, then Assumption 2 will be satisfied when Γ has small enough entries (because $H = E$). Hence, the control parameters can be chosen in the following three steps. First, choose K so that H satisfies the preceding conditions. Second, choose L such that Assumption 1 is satisfied. Third, choose Γ to have small enough entries so that Assumption 2 is also satisfied. Therefore, taken together, Assumptions 1–2 are a time-varying robustified analog of the requirements from the emulation conditions in event-triggered control. These assumptions will be used in the second part of our proof of our theorem, to establish the exponential convergence conclusion of our theorem. See Appendix A for ways to check whether Assumption 2 is satisfied.

Given K and Γ satisfying the requirements from Assumption 2, we use the function

$$\Omega_0(t,s) = \Phi_{A_0}(t,s) + \int_s^t \Phi_{A_0}(t,m)B_0(m)K(m)\mathrm{d}m, \tag{6}$$

and we consider any constant $\nu > 0$ such that

$$\sup\{|I - \Omega_0^{-1}(t,s)| : 0 \leq s \leq t \leq s+\nu\} \leq \Gamma, \tag{7}$$

where Γ is from Assumption 2 and where the inverse values Ω_0^{-1} will exist for small enough $\nu > 0$ because $\Omega_0(s,s) = I$ for all $s \geq 0$, and because the boundedness of A_0, B_0, and K implies that $\sup\{\|(\partial\Omega_0/\partial t)(t,s)\| : 0 \leq s \leq t \leq s+\nu\}$ is bounded for each $\nu > 0$. See Appendix B for ways to find constants $\nu > 0$ to satisfy (7), including a method based on factoring fundamental solutions. In Section 5, we prove that our constant $\nu > 0$ that satisfies (7) is a lower bound on the intervals between the event triggering times t_i, so the Zeno phenomenon does not occur.

Fixing any constant $\nu > 0$ satisfying (7) and V satisfying the requirements from Assumption 2, and letting $\underline{v}$ denote the smallest entry of the constant vector $\underline{V} > 0$ from Assumption 2, and letting c_* and g be positive constants such that

$$\|z(t)\| \leq c_* e^{-g(t-s)}\|z(s)\| \tag{8}$$

holds along all solutions of (2) for all $s \geq 0$ and $t \geq s$ (so g is the rate of global exponential convergence in Assumption 1), and using the notation

$$\mathcal{B} = (I + \Gamma)\, E_\nu, \tag{9}$$

where

$$E_\nu = \sup\{|\Phi_{A_0}(t,s)L(s)| : 0 \leq s \leq t \leq s+\nu\} \tag{10}$$

where Γ and L are from Assumptions 1–2, our last assumption is as follows, where C is the matrix used in (1):

Assumption 3. The constants

$$\begin{aligned} G_1 &= \tfrac{2c_*}{g}\left(\|A_\delta\|_\infty + \|B_\delta K\|_\infty\right) \text{ and} \\ G_2 &= \tfrac{2}{p\underline{v}}\left(\left|\left|V^\top|B_0K|\mathcal{B}|C|\right|\right|_\infty \nu + \left|\left|V^\top|LC|\right|\right|_\infty\right) \end{aligned} \tag{11}$$

are such that the inequality

$$G_1 G_2 < 1 \tag{12}$$

is satisfied. □

Remark 1. Condition (12) is a small-gain condition that we use in the second part of the proof of our theorem in Section 5; see Remark 4, and see [10] for background on small-gain methods. Although larger g values in the G_1 formula can reduce G_1, the price to pay is to change L in Assumption 1, which would produce changes in the $\mathcal{B}$ in the G_2 formula; see (9)-(10). Hence, Assumption 3 also illustrates the trade-off between convergence rates and gains in Assumption 1. In a similar way, while changing K in Assumption 2 may allow larger decay rates $p > 0$ in our condition (5) in Assumption 2 and so increase the denominator of G_2, the price to pay could be to increase G_1. □

4. Event-triggered control design

In terms of the preceding matrices and constants and the matrices (9), and continuing our notation $A = A_0 + A_\delta$ and $B = B_0 + B_\delta$, we are now ready to define our event-triggered control. Our event-triggered feedback control and the corresponding event-triggering times t_i are defined by

$$u(t) = K(t)\hat{x}(t_i) \text{ for all } t \in [t_i, t_{i+1}) \text{ and } i \geq 0, \tag{13}$$

where $t_0 = 0$, and where for integers $i \geq 0$, we have

(a) $\dot{x}(t) = A(t)x(t) + B(t)K(t)\hat{x}(t_i)$ if $t \in (t_i, t_{i+1})$,
(b) $\dot{\hat{x}}(t) = A_0(t)\hat{x}(t) + B_0(t)K(t)\hat{x}(t_i) + L(t)[C\hat{x}(t) - y(t)]$ if $t \in (t_i, t_{i+1})$,
(c) the inequality

$$\begin{aligned} &|\hat{x}(t) - \hat{x}(t_i)| \leq \\ &\Gamma|\hat{x}(t)| + \mathcal{B}\int_{\max\{0,t-\nu\}}^t |C\hat{x}(\ell) - y(\ell)|\mathrm{d}\ell \end{aligned} \tag{14}$$

is satisfied for all $t \in [t_i, t_{i+1})$, and
(d) for each i such that $t_i < +\infty$, we have

$$\begin{aligned} t_{i+1} = \sup\Big\{ &s \geq t_i : |\hat{x}(r) - \hat{x}(t_i)| \leq \Gamma|\hat{x}(r)| \\ &+ \mathcal{B}\int_{\max\{0,r-\nu\}}^r |C\hat{x}(\ell) - y(\ell)|\mathrm{d}\ell \text{ for all } r \in [t_i, s]\Big\}, \end{aligned} \tag{15}$$

where $|\cdot|$ denotes vectors of absolute values as explained in Section 2, $\mathcal{B}$ is from (9), the constant $\nu > 0$ satisfies the requirements from Section 3, and $L(t)$ was specified in Assumption 1. The system (a)–(d) is an event-triggered dynamics that resets the control values at the times t_i, using the following inductive argument.

Starting at time $t_0 = 0$, we choose $u(t) = K(t)\hat{x}(0)$. Then, we continue to use the control formula $u(t) = K(t)\hat{x}(0)$ as long as

$$\begin{aligned} &|\hat{x}(t) - \hat{x}(0)| \leq \\ &\Gamma|\hat{x}(t)| + \mathcal{B}\int_{\max\{0,t-\nu\}}^t |C\hat{x}(\ell) - y(\ell)|\mathrm{d}\ell \end{aligned} \tag{16}$$

continues to hold. This yields an interval $[0, t_*]$ along which the control takes the values $u(t) = K(t)\hat{x}(0)$, and the proof of our theorem will show that $t_* \geq \nu$. Then we change the control formula to $u(t) = K(t)\hat{x}(t_1)$, where t_1 is the supremum from (d) with the choice $i = 0$, if $t_1 < +\infty$. We repeat this process inductively, with t_0 replaced by t_1, then by t_2, and so on, to define the control values and triggering times t_i for all $t \geq 0$. Hence, (a)–(d) provide a recursively defined event-triggered control, whose triggers are computed from values of the observer $\hat{x}$. See Remark 3 for ways to implement the preceding event-triggered algorithm. Our theorem is then:

Theorem 1. *Let Assumptions 1–3 hold, and let K, L, Γ, and ν satisfy the requirements above. Then we can find positive constants r_1 and r_2 such that all solutions of the closed-loop system given by (a)–(d) satisfy $\|x(t)\| \leq r_1 e^{-r_2 t}\|x(0)\|$ for all $t \geq 0$.* □

Remark 2. The preceding theorem is new, even in the special case where A_δ and B_δ are zero. This is because of our ability to achieve event-triggered output feedback stabilization with time-varying coefficients A_0 and B_0. □

Remark 3. We can implement the event-triggered control (a)–(d) by extrapolating; see Section 6, where we implemented our method by extrapolation. Alternatively, Theorem 1 remains true if we fix any constant $T \geq \nu$ (with ν again chosen as in Section 3) and then replace (c)–(d) by (c′) the inequality

$$|\hat{x}(t-T)-\hat{x}(t_i)| \leq \Gamma|\hat{x}(t-T)| + \mathcal{B}\int_{\max\{0,t-T-\nu\}}^{t-T} |C\hat{x}(\ell)-y(\ell)|\mathrm{d}\ell \tag{14′}$$

is satisfied for all $t \in [t_i+T, t_{i+1}+T)$, and

(d′) for each $i \in \mathbb{Z}_0$, we have $0 \leq t_{i+1}-t_i \leq T$. In addition, if i is such that $t_{i+1} < t_i + T$, then we have

$$t_{i+1} = \sup\Big\{s \geq t_i : |\hat{x}(r-T)-\hat{x}(t_i)| \leq \Gamma|\hat{x}(r-T)| + \mathcal{B}\int_{\max\{0,r-\nu-T\}}^{r-T}|C\hat{x}(\ell)-y(\ell)|\mathrm{d}\ell \text{ for all } r \in [t_i+T, s+T]\Big\}. \tag{15′}$$

With the preceding changes, the event-triggered control is implemented as follows. At time $t_0 = 0$, we choose $u(0) = K(0)\hat{x}(0)$, and then we use the control values $u(t) = K(t)\hat{x}(0)$ up to time $t = t_0 + T = T$, or up to the infimum of the times $t > T$ when the value $t - T$ fails to satisfy (14′) if such a violation of (14′) occurs, whichever occurs first. We call this time t_1. At that time t_1, we switch to using the control values $u(t) = K(t)\hat{x}(t_1)$. Then we repeat this process with $i = 0$ replaced by $i = 1$, and argue inductively to obtain control values and triggering times that are defined for all times $t \geq 0$. The fact that Theorem 1 remains true with the preceding changes follows by replacing t throughout the first part of the proof of the theorem below by $t - T$. Hence, only measurements of $\hat{x}$ and of the output y up to time $t - T$ are needed to monitor the event trigger at times t. Using the change of variable $s = t - T$ in (14′), it then follows that (14) remains true for all $t \in [t_i, t_{i+1})$ for values $i \geq 0$, so the second part of the proof of the theorem below remains valid with the preceding changes in (c)–(d). Moreover, with the preceding changes, we still obtain the lower bound $t_{i+1} - t_i \geq \nu$ on the intersample intervals for all i.

5. Proof of Theorem 1

The proof has two parts. In the first part, we use our condition (7) on the constant $\nu > 0$ to show that the Zeno phenomenon does not occur. In the second part, we use Assumptions 1–3 to show that the global exponential stability conclusion of the theorem holds.

First part. Letting ν be the constant we defined above, we prove that the inter-event times $t_{i+1} - t_i$ are bounded below by ν, i.e., if there are any finite triggering times $t_i > 0$, then either (A) there are only a finite number of finite instants $t_0, \ldots, t_j$ and $\min_{l\in\{0,\ldots,j\}}(t_{l+1} - t_l) \geq \nu$ or (B) there are infinitely many finite instants t_i and $\inf_{l\in\mathbb{Z}_0}(t_{l+1} - t_l) \geq \nu$. (The case where there are no trigger times gives $t_1 = +\infty$ and $u(t) = K(t)\hat{x}(0)$ for all $t \geq 0$.)

For any $i \in \mathbb{Z}_0$ such that $t_i < +\infty$, we apply the method of variation of parameters to the equation in (b) over $[t_i, t)$ with $t \in [t_i, t_i + \nu]$ with the initial state $\hat{x}(t_i)$ to get

$$\hat{x}(t) = \mathcal{G}(t, t_i) + \left[\Phi_{A_0}(t, t_i) + \int_{t_i}^{t} \Phi_{A_0}(t, \ell)B_0(\ell)K(\ell)\mathrm{d}\ell\right]\hat{x}(t_i), \tag{17}$$

where

$$\mathcal{G}(t, t_i) = \int_{t_i}^{t} \Phi_{A_0}(t, \ell)L(\ell)[C\hat{x}(\ell) - y(\ell)]\mathrm{d}\ell. \tag{18}$$

Hence, $\hat{x}(t_i) = \Omega_0^{-1}(t, t_i)[\hat{x}(t) - \mathcal{G}(t, t_i)]$ for all $t \in [t_i, t_i + \nu]$, which is equivalent to

$$\hat{x}(t) - \hat{x}(t_i) = \left[I - \Omega_0^{-1}(t, t_i)\right]\hat{x}(t) + \Omega_0^{-1}(t, t_i)\mathcal{G}(t, t_i) \tag{19}$$

for all $t \in [t_i, t_i + \nu]$. Hence, (7) gives

$$|\hat{x}(t) - \hat{x}(t_i)| \leq \Gamma|\hat{x}(t)| + |\Omega_0^{-1}(t, t_i)\mathcal{G}(t, t_i)| \tag{20}$$

for all $t \in [t_i, t_i + \nu]$.

Since our formula (18) for $\mathcal{G}$ and our choice (10) of E_ν give

$$|\mathcal{G}(t, t_i)| \leq E_\nu \int_{t_i}^{t} |C\hat{x}(\ell) - y(\ell)|\mathrm{d}\ell, \tag{21}$$

and since (7) gives $|\Omega_0^{-1}(t, t_i)| \leq \Gamma + I$, it follows from our choice (9) of $\mathcal{B}$ that we have

$$|\Omega_0^{-1}(t, t_i)\mathcal{G}(t, t_i)| \quad \leq \quad \mathcal{B}\int_{\max\{0,t-\nu\}}^{t} |C\hat{x}(\ell) - y(\ell)|\mathrm{d}\ell \tag{22}$$

for all $t \in [t_i, t + \nu]$. Using (22) to upper bound the second right side term in (20), it follows that the inequality (14) holds for all $t \in [t_i, t_i + \nu]$, which gives $t_{i+1} \geq t_i + \nu$.

Second part. We prove the global exponential stability of the 0 equilibrium of the closed-loop system (a)–(d). In what follows, all equalities and inequalities should be understood to hold for all $t \geq 0$, unless otherwise indicated.

Let $\tilde{x}(t) = \hat{x}(t) - x(t)$ and $G = A_0 + LC$. Then (a)–(b) give

$$\begin{aligned} \dot{\tilde{x}}(t) &= G(t)\tilde{x}(t) - A_\delta(t)x(t) - B_\delta(t)K(t)\hat{x}(\sigma(t)) \\ &= [G(t) + A_\delta(t)]\tilde{x}(t) \\ &\quad - A_\delta(t)\hat{x}(t) - B_\delta(t)K(t)\hat{x}(\sigma(t)) \end{aligned} \tag{23}$$

for all $t \geq 0$, where $\sigma(t)$ is the largest of the times t_i such that $t_i \leq t$. Therefore, by applying the method of variation of parameters to the last equality in (23), it follows from Assumption 1 that (23) satisfies an exponential ISS estimate of the form

$$\|\tilde{x}(t)\| \leq \max\{\beta_1(\|\tilde{x}(s)\|, t - s), \gamma_1(\|\hat{x}\|_{[\sigma(s),t]})\} \tag{24}$$

for all $s \geq 0$ and $t \geq s$ and for a suitable function $\beta_1 \in \mathcal{KL}$ and the class $\mathcal{K}_\infty$ function $\gamma_1(s) = G_1 s$, where G_1 was defined in (11), and where the exponential property of the ISS means that there are positive constants c_1 and c_2 such that $\beta_1(s, t) = c_1 s e^{-c_2 t}$ for all $s \geq 0$ and $t \geq 0$. Here we used the fact that (8) implies that the fundamental matrix for (2) satisfies $||\Phi_{A+LC}(t, s)|| \leq c_* e^{-g(t-s)}$.

Also, setting $H = A_0 + B_0 K$ and $\hat{\mu}(t) = \hat{x}(t_i) - \hat{x}(t)$ for all $t \in [t_i, t_{i+1})$ and $i \geq 0$, we have

$$\begin{aligned} \dot{\hat{x}}(t) &= H(t)\hat{x}(t) + B_0(t)K(t)\hat{\mu}(t) + L(t)C\tilde{x}(t) \\ &= [R_H(t) - N_H(t)]\hat{x}(t) \\ &\quad + B_0(t)K(t)\hat{\mu}(t) + L(t)C\tilde{x}(t). \end{aligned} \tag{25}$$

We next introduce the comparison system

$$\left\{ \begin{aligned} \dot{\overline{x}}(t) &= R_H(t)\overline{x}(t) - N_H(t)\underline{x}(t) \\ &\quad + (B_0(t)K(t)\hat{\mu}(t))^+ + (L(t)C\tilde{x}(t))^+ \\ \dot{\underline{x}}(t) &= R_H(t)\underline{x}(t) - N_H(t)\overline{x}(t) \\ &\quad - (B_0(t)K(t)\hat{\mu}(t))^- - (L(t)C\tilde{x}(t))^- \end{aligned} \right. \tag{26}$$

which we use as an interval observer for $\hat{x}$. We refer to (26) as an interval observer, because (as we show later in the proof) it will satisfy $\underline{x}(t) \leq \hat{x}(t) \leq \overline{x}(t)$ for all $t \geq 0$ and so provides an interval $[\underline{x}_i(t), \overline{x}_i(t)]$ containing each component $\hat{x}_i(t)$ for all $t \geq 0$ and $i = 1, 2 \ldots, n$. We assume

$$\underline{x}(0) < 0 < \overline{x}(0) \text{ and } \underline{x}(0) < \hat{x}(0) < \overline{x}(0). \tag{27}$$

Since $Y(t) = (\overline{x}(t), -\underline{x}(t))$ is a solution of a dynamics of the form

$$\dot{Y}(t) = \mathcal{H}(t)Y(t) + \mathcal{P}(t) \tag{28}$$

for some matrix-valued functions $\mathcal{H}$ and $\mathcal{P}$ having piecewise continuous entries such that $\mathcal{H}(t)$ is Metzler for all $t \geq 0$ and $\mathcal{P}(t) \geq 0$ for all $t \geq 0$, [22, Lemma 1] implies that

$$\underline{x}(t) \leq 0 \leq \overline{x}(t) \tag{29}$$

for all $t \geq 0$. Similar reasoning implies that $\overline{x}(t) - \hat{x}(t) \geq 0$ and $\hat{x}(t) - \underline{x}(t) \geq 0$ for all $t \geq 0$; this follows by applying [22, Lemma 1] to the $2n$ dimensional dynamics for $(\overline{x}(t) - \hat{x}(t), \hat{x}(t) - \underline{x}(t))$. Hence, for all $t \geq 0$, we obtain

$$\underline{x}(t) \leq 0 \leq \overline{x}(t) \text{ and } \underline{x}(t) \leq \hat{x}(t) \leq \overline{x}(t). \tag{30}$$

For the preceding initial conditions, set $x_\star(t) = \bar{x}(t) - \underline{x}(t)$. Then (30) gives $\underline{x}(t) - \bar{x}(t) \le \hat{x}(t) \le \bar{x}(t) - \underline{x}(t)$ and so also

$$|\hat{x}(t)| \le x_\star(t). \tag{31}$$

Simple calculations give

$$\begin{array}{rcl} \dot{x}_\star(t) & = & (R_H(t) + N_H(t))x_\star(t) \\ & & + |B_0(t)K(t)\hat{\mu}(t)| + |L(t)C\tilde{x}(t)|. \end{array} \tag{32}$$

Consider the function $W(t, x_\star) = V^\top(t)x_\star$, where V is from Assumption 2. By (c) and (32), it satisfies

$$\begin{array}{rcl} \dot{W}(t) & = & \dot{V}^\top(t)x_*(t) + V^\top(t)(R_H(t) + N_H(t))x_\star(t) \\ & & + V^\top|B_0(t)K(t)\hat{\mu}(t)| + V^\top(t)|L(t)C\tilde{x}(t)| \\ & \le & \dot{V}^\top(t)x_*(t) + V^\top(t)(R_H(t) + N_H(t))x_\star(t) \\ & & + V^\top(t)|B_0(t)K(t)|\big(\Gamma|\hat{x}(t)| \\ & & + \mathcal{B}\int_{\max\{0,t-\nu\}}^t C^\sharp(\ell)\mathrm{d}\ell\big) + V^\top|L(t)C\tilde{x}(t)| \end{array} \tag{33}$$

for all $t \ge 0$ along solutions of (32), where the notation R_H and N_H is as defined in Section 2, $\mathcal{B}$ was defined in (9), $C^\sharp(\ell) = C\hat{x}(\ell) - y(\ell)$ and $\dot{W}(t)$ means $(d/dt)W(t, x_*(t))$. Using (5), (31), and (33), we get

$$\begin{array}{rcl} \dot{W}(t) & \le & -pW(t, x_\star(t)) + V^\top(t)|L(t)C\tilde{x}(t)| \\ & & + V^\top(t)|B_0(t)K(t)|\mathcal{B}\int_{\max\{0,t-\nu\}}^t C^\sharp(\ell)\mathrm{d}\ell \\ & \le & -pW(t, x_\star(t)) + \Xi(t), \text{ where} \\ \Xi(t) & = & V^\top(t)|B_0(t)K(t)|\mathcal{B}|C|\int_{\max\{0,t-\nu\}}^t |\tilde{x}(\ell)|\mathrm{d}\ell \\ & & + V^\top|L(t)C\tilde{x}(t)|, \end{array} \tag{34}$$

where the first inequality in (34) used the nonnegative valuedness of $x_*(t)$ (which follows from (31)) to maintain the inequality from (5) when (5) is right multiplied by $x_*(t)$.

By applying the method of variation of parameters to

$$\dot{W}(t) \le -pW(t, x_\star(t)) + \Xi(t) \tag{35}$$

from (34), it follows from the formula (34) for Ξ that the x_* dynamics satisfies an exponential ISS estimate of the form

$$\begin{array}{l} |x_*(t)| \le \\ \max\{\beta_2(|x_*(s)|, t-s), \gamma_2(|\tilde{x}|_{[\max\{0,s-\nu\},t]})\} \end{array} \tag{36}$$

for all $s \ge 0$ and $t \ge s$ and for a function $\beta_2 \in \mathcal{KL}$ (having the form $\beta_2(s, t) = d_1 s e^{-d_2 t}$ for suitable positive constants d_1 and d_2), because of the exponential ISS estimate (35) and the bound $\|W(s, x_*(s))\| \le \|\bar{V}|x_*(s)|\|$, where $\bar{V}$ is the upper bound on V from (4)) and $\gamma_2(s) = G_2 s$, where G_2 was defined in (11). We now use (31) to upper bound $|\hat{x}|$ in the ISS estimate (24) to obtain the new estimate

$$\begin{array}{l} \|\tilde{x}(t)\| \le \\ \max\{\beta_1(\|\tilde{x}(s)\|, t-s), \gamma_1(\|x_*\|_{[\max\{0,s-\nu\},t]})\} \end{array} \tag{37}$$

for all $s \ge 0$ and $t \ge s$. Then, we use the small-gain condition $G_1 G_2 < 1$ from Assumption 3 to check that the looped ISS estimate (36)-(37) is such that $\gamma_1(\gamma_2(s)) < s$ for all $s > 0$. It then follows from the proof of the small-gain theorem (e.g., from [10, p. 61] or the proof of [23, Theorem 2.6]) that the $(x_*, \tilde{x})$ dynamics are globally exponentially stable to 0 on $\mathbb{R}^{2n}$. The conclusion of Theorem 1 now follows because we can assume that $\bar{x}(0) \le \mathcal{M}|x(0)|$ and $\underline{x}(0) \ge -\mathcal{M}|x(0)|$ for a large enough constant $\mathcal{M} > 0$, which imply that our condition (31) gives $\|x(t)\| = \|\hat{x}(t) - \tilde{x}(t)\| \le \|\hat{x}(t)\| + \|\tilde{x}(t)\| \le \|x_*(t)\| + \|\tilde{x}(t)\| \le 2\|(x_*(t), \tilde{x}(t))\|$ for all $t \ge 0$ and $\|(x_*(0), \tilde{x}(0))\| \le (4\mathcal{M} + 1)\|x(0)\|$, so we can convert the exponential stability estimate for $(x_*, \tilde{x})$ into the required exponential stability estimate for $x(t)$.

Remark 4. Our small-gain argument from the previous proof differs significantly from standard small-gain approaches to event triggering, because we use a small-gain condition between $\tilde{x}$ and x_*, instead of between the original system and the event triggering rule. □

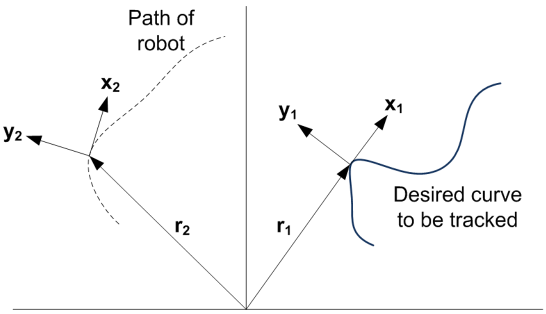

Fig. 1. Curve Tracking Frames and Positions from [25].

6. Illustrations

6.1. Output feedback event-triggered control

In this subsection, we illustrate Theorem 1, using a benchmark two-dimensional (i.e., planar) curve tracking dynamical system from [24,25]. While simpler than more complex ship models, or the analogous 3D curve tracking model from [25,26], it illustrates the value of Theorem 1 for using event-triggering to eliminate the need to continuously adjust the control values. We consider the system

$$\left\{ \begin{array}{rcl} \dot{\rho}(t) & = & -\sin(\phi(t)) \\ \dot{\phi}(t) & = & \frac{\kappa\cos(\phi(t))}{1+\kappa\rho(t)} + u(t) \\ y(t) & = & \rho(t) \end{array} \right. \tag{38}$$

which models curve tracking by a unit speed surface marine robot with a gyroscopic control u. In (38), the available measurement ρ is the distance between the marine robot and the closest point (i.e., projection) on the curve being tracked (where we assume as in [25] that the closest point is unique at each time), ϕ is the heading angle (measuring the difference between the angles of the tangent lines of the path of the marine robot and of the path being traced out by the closest point on the curve being tracked), and κ is the curvature at each time. See [25] for a derivation of the model (38). Also, see Fig. 1 for the position and frame $(\mathbf{r_1}, \mathbf{x_1}, \mathbf{y_1})$ on the boundary curve being tracked at the closest point, and the position and frame $(\mathbf{r_2}, \mathbf{x_2}, \mathbf{y_2})$ for the vehicle, where $\rho = \|\mathbf{r_1} - \mathbf{r_2}\|$, and ϕ is the angle between the tangent vector $\mathbf{x_1}$ at the projection point on the curve being tracked and the tangent vector $\mathbf{x_2}$ on the curve being traced out by the robot at each time. We assume for simplicity that κ is a positive constant.

The linear approximation of (38) around any choice of the reference trajectory $(\rho_r(t), \phi_r(t))$ is

$$\left\{ \begin{array}{rcl} \dot{\rho}_a(t) & = & a_{12}(t)\phi_a(t) \\ \dot{\phi}_a(t) & = & a_{21}(t)\rho_a(t) + a_{22}(t)\phi_a(t) + u(t) \\ y(t) & = & \rho_a(t), \end{array} \right. \tag{39}$$

where

$$\begin{array}{l} a_{12}(t) = -\cos(\phi_r(t)),\ a_{21}(t) = -\frac{\kappa^2\cos(\phi_r(t))}{(1+\kappa\rho_r(t))^2}, \\ \text{and } a_{22}(t) = -\frac{\kappa\sin(\phi_r(t))}{1+\kappa\rho_r(t)}. \end{array} \tag{40}$$

Let us consider the reference trajectory (ρ_r, ϕ_r), where

$$\rho_r(t) = \frac{1}{\kappa}\left(1 - \frac{t\Delta_*}{1+t}\right) \text{ and } \phi_r(t) = \arcsin\left(\frac{\Delta_*}{\kappa(1+t)^2}\right). \tag{41}$$

The physical meaning of the constant $\Delta_* \in [0, \min\{1, \kappa\})$ is that it determines how fast the robot is traveling towards the curve that is being tracked. For this reference trajectory, $(1 - \Delta_*)/\kappa$ is the infimum of the distance between the position of the robot and the projection on the curve being tracked. Then (39)-(40) give

$$\begin{aligned} &a_{12}(t) = \mathcal{A}_1(t) - 1,\ a_{21}(t) = -\tfrac{\kappa^2}{4} + \mathcal{A}_2(t),\ \text{and} \\ &a_{22}(t) = \mathcal{A}_3(t),\ \text{where } \mathcal{A}_1(t) = 1 - \left(1 - \tfrac{\Delta_*^2}{\kappa^2(1+t)^4}\right)^{1/2}, \\ &\mathcal{A}_2(t) = \kappa^2 \left(\tfrac{1}{4} - \frac{\sqrt{1 - \frac{\Delta_*^2}{\kappa^2(1+t)^4}}}{\left(2 - \frac{t\Delta_*}{1+t}\right)^2} \right),\ \text{and} \\ &\mathcal{A}_3(t) = -\tfrac{\Delta_*}{(1+t)^2} \tfrac{1}{2 - \frac{t\Delta_*}{1+t}}. \end{aligned} \tag{42}$$

Let us choose $\kappa = 2$. This produces the dynamics

$$\left\{ \begin{array}{rcl} \dot{\rho}_a(t) & = & (\mathcal{A}_1(t) - 1)\phi_a(t) \\ \dot{\phi}_a(t) & = & -(1 - \mathcal{A}_2(t))\rho_a(t) + \mathcal{A}_3(t)\phi_a + u(t) \\ y(t) & = & \rho_a(t). \end{array} \right. \tag{43}$$

The change of coordinates $(x_1(t), x_2(t)) = (\rho_a(t), \rho_a(t) - \phi_a(t))$ produces the dynamics $\dot{x}(t) = A(t)x(t) + Bu$ with output $y(t) = Cx(t)$, where

$$A(t) = \begin{bmatrix} \mathcal{A}_1(t) - 1 & 1 - \mathcal{A}_1(t) \\ \mathcal{A}_4(t) & 1 - \mathcal{A}_1(t) + \mathcal{A}_3(t) \end{bmatrix}, \tag{44}$$

$B = [0, -1]^\top$, $C = [1, 0]$, and $\mathcal{A}_4 = \mathcal{A}_1 - \mathcal{A}_2 - \mathcal{A}_3$.

Then simple Mathematica calculations show that the requirements of Assumptions 1–3 are satisfied with $A_\delta = 0$, $B_\delta = 0$, $V = [1, 2]^\top$, $K = [0, 1.75]$, each entry of Γ being 0.1, $L = [-2, -5]^\top$, and $p = 0.01$ when $\Delta_* = 0.1$. The preceding choices of V, p, K, L, and Γ were obtained by first finding constant choices of V, p, K, L and Γ for which our assumptions are satisfied in the special case where $\Delta_* = 0$ (and with a constant choice of H that is both Metzler and Hurwitz), and then by choosing $\Delta_* > 0$ to be a small enough constant such that the requirements of our assumptions are still met with these choices of V, p, K, L, and Γ. For instance, to check that Assumption 1 is satisfied, we solved the Riccati equation $PM + M^\top P = -I$ for P with the choice $M = A + LC$ in the $\Delta_* = 0$ case, and then we checked that $\Delta_* = 0.1$ was small enough so that $V_0(z) = z^\top Pz$ is a quadratic Lyapunov function for $\dot{z}(t) = (A(t) + LC)z(t)$. Then the requirement (B.1) from Lemma B.1 in Appendix B is satisfied with $\nu = 0.026$. Hence, (7) is satisfied, so Theorem 1 applies in the special case where A_δ an B_δ are both the zero matrices.

If we replace (41) by the reference trajectory

$$\rho_r(t) = \frac{1}{\kappa}(1 - 0.1\sin(t)) \text{ and } \phi_r(t) = \arcsin\left(\frac{\cos(t)}{10\kappa}\right) \tag{45}$$

and replace V, p, Γ, and ν by $V = [1, 3.7]^\top$, $p = 0.001$,

$$\Gamma = \begin{bmatrix} 0.6075 & 0.648 \\ 0.081 & 0.243 \end{bmatrix} \tag{46}$$

and $\nu = 0.2125$, respectively, and keep the rest of the dynamics the same, then (7) is again satisfied. This can be checked by noting that

$$\sup\{|I - \Omega_0^{-1}(t, s)| : s \in [0, 2\pi], t \in [s, s + \nu]\} \le \Gamma, \tag{47}$$

and then using the argument from Appendix B for cases where $A(t)$ is periodic. The entries of Γ in (46) and ν were chosen using the following two step process. In the first step, the entries of Γ were chosen as the largest ones for which the requirements of Assumption 2 were satisfied with the preceding choices of A, B, V, K, and p. Then, in the second step, $\nu > 0$ was chosen to be the largest value such that (7) is satisfied with the preceding choices of A, B, K, and $\Gamma = [\Gamma_{ij}]$. However, with the preceding choices, our sufficient condition (B.1) from the proof of Lemma B.1 is not satisfied, because its left side with $\bar{b} = \|BK\|$ and $\bar{a} = \|A\|_\infty$ is $2.07515 > \min\{\Gamma_{11}, \Gamma_{12}, \Gamma_{21}, \Gamma_{22}, 1\} = 0.081$. This illustrates how numerical techniques (such as the alternative methods from Appendix B) can allow cases where (B.1) is violated but where our method still applies.

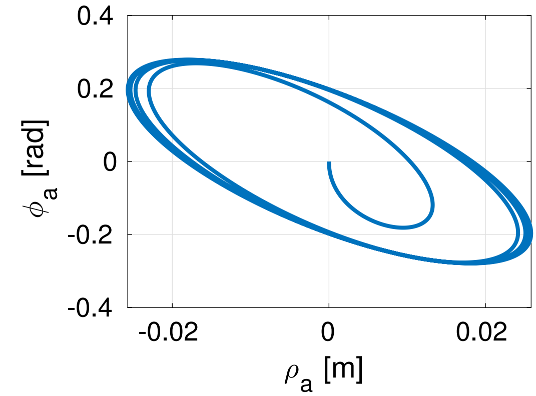

Fig. 2. Curve Tracking in Periodic Case, showing Convergence of State Vector to Desired Elliptic Curve using Positive Systems Based Event-Triggered Control from Theorem 1: Phase Plane.

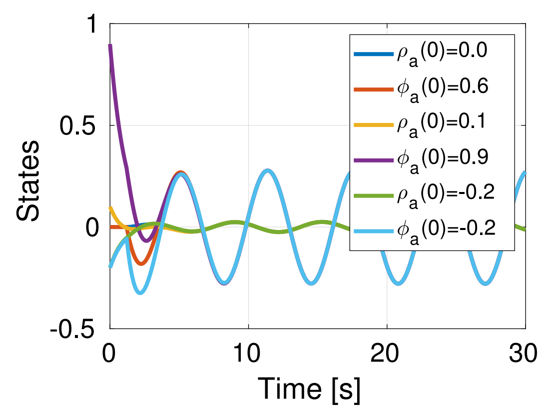

Fig. 3. Tracking in Periodic Case, showing Convergence to Desired Oscillatory Curves using Positive Systems Based Event-Triggered Control from Theorem 1: States from Theorem 1.

In Figs. 2–3, we plot MATLAB simulations that we obtained in the preceding periodic case with the preceding parameter values using the event-triggered control from our theorem (i.e., (a)–(d) above) applied to (43). In the top figure, we used $\rho_a(0) = \phi_a(0) = 0.1$ as the initial state. In Fig. 3, we plot the solutions that we obtained for different initial states $(\rho_a(0), \phi_a(0))$. Since the plots show convergence to the reference trajectory (45), they illustrate the value of our theorem, and they demonstrate the benefits of our event-triggered control designs.

The preceding cases are beyond the scope of works for time-invariant systems such as [8], because of our time-varying coefficient $A(t)$, unless $\Delta_* = 0$ in our reference trajectory (41). In the special case where $\Delta_* = 0$, the matrix A is constant, and in that $\Delta_* = 0$ case, the example would be covered by [8] if we instead had $C = I$. Therefore, we next compare the lower bound ν that we would obtain from our method with the lower bound ν that could be obtained from [8, Corollary IV.1] in the $\Delta_* = 0$ and $C = I$ case. When $\Delta_* = 0$, our assumptions and our requirement (B.1) from Lemma B.1 are satisfied with $\nu = 0.0925$ and the same choices of the other parameters that we used in our treatment of the $\Delta_* = 0.1$ case. On the other hand, if we apply [8, Corollary IV.1] with the same set of parameters (using

$\sigma = \min\{\Gamma_{ij} : 1 \le i \le n, 1 \le j \le n\} = 0.1$ in [8, Corollary IV.1], which corresponds to our trigger condition $|e| \le \Gamma|x|$), then we would have gotten $\nu = 0.0592$, so our method provides a larger lower bound ν on the inter-sample times, and therefore ensures less frequent event triggers.

6.2. Robustness

We next illustrate Theorem 1 using the special case

$$\begin{cases} \dot{x}_1(t) &= (1+\delta_1(t))x_1(t) + \frac{1}{2}(1+\delta_2(t))x_2(t) + u \\ \dot{x}_2(t) &= \frac{3}{2}(1+\delta_3(t))x_1(t) + u \end{cases} \tag{48}$$

of (1) with $B_0 = [1, 1]^\top$, $B_\delta = 0$, $C = I$,

$$A_0 = \begin{bmatrix} 1 & \frac{1}{2} \\ \frac{3}{2} & 0 \end{bmatrix}, \text{ and } A_\delta(t) = \begin{bmatrix} \delta_1 & \frac{1}{2}\delta_2 \\ \frac{3}{2}\delta_3 & 0 \end{bmatrix}, \tag{49}$$

where x_1 and x_2 are valued in $\mathbb{R}$, the piecewise continuous bounded unknown functions δ_i represent uncertainty, and u is the real valued input, which agrees with the example in [20] when each δ_i is the zero function. Then, using the notation $K = [K_1,\ K_2]$, our assumptions will be satisfied when the supremum of the δ_i's and the entries of $\Gamma > 0$ are small enough, provided

$$H = \begin{bmatrix} 1+K_1 & \frac{1}{2}+K_2 \\ \frac{3}{2}+K_1 & K_2 \end{bmatrix} \tag{50}$$

is Hurwitz and Metzler (again by [19, Lemma 2.3, p.41]). We will therefore choose $K_1 = -4/3$ and $K_2 = -1/3$. Then simple Mathematica calculations show that the requirements of Theorem 1 are satisfied when $\sup\{|\delta_i(t)| : t \ge 0\} \le 0.01$ for all i, by choosing $L = [l_{ij}]$ with $l_{11} = -1.1$, $l_{12} = -0.5$, $l_{21} = -0.5$, and $l_{22} = -0.1$, and $\nu = 0.02$, and each entry of Γ to be 0.045, because these choices ensure that our assumptions and (7) hold. Moreover, when the δ_i's are 0, we can satisfy the requirements with $\nu = 0.122$ with all other parameters as before. This gives the lower bound $\nu = 0.122$ on the intersampling times $t_{i+1} - t_i$.

In the special case of the preceding example where each δ_i is the zero function, the system (48) is covered by the event-triggered results from [8]. If we had instead used [8, Corollary IV.1] to obtain a lower bound on the $t_{i+1} - t_i$'s (using $\sigma = \min\{\Gamma_{ij} : 1 \le i \le n, 1 \le j \le n\} = 0.045$ in [8, Corollary IV.1], which corresponds to our trigger condition $|e| \le \Gamma|x|$), then we would have gotten $\nu = 0.0811$ in the case where the δ_i's are the zero function. Hence, our method again provides a larger ν and the potential advantage of ensuring less frequent control recomputations.

Fig. 4 shows MATLAB simulations of (48) that implement the event-triggered controller from Theorem 1, with a 20 second time horizon using the above parameter values with the δ_i's taken to be the constant values 0.01. For this time horizon, our controller from Theorem 1 produced 73 sample times when the control was recomputed.

7. Conclusion

In this paper, we used the theory of positive linear time-varying systems and interval observers, along with small-gain techniques, to tackle the robust, event-triggered, output-feedback control of linear time-varying systems. Our design method was motivated by the need to only infrequently recompute control values in marine robotic and other applications, instead of frequently changing control values. It has been shown how to guarantee robust global exponential stability properties for large classes of linear time-varying systems with output feedback and uncertainty in the coefficient matrices. The efficacy of the new proposed framework is illustrated through explicit quantification of uncertainty and implementation in a marine robotic example.

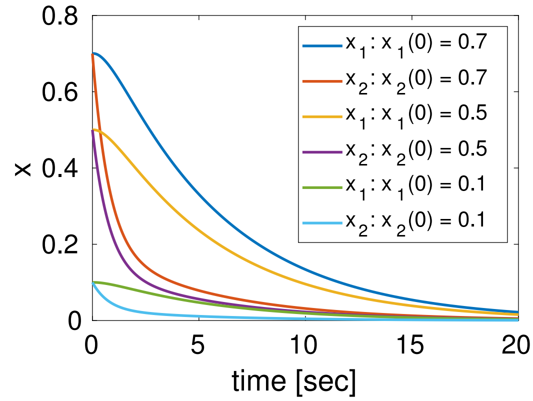

Fig. 4. Positive Systems Approach in Unperturbed Case, illustrating the Capability of our Event-Triggered Control from Theorem 1 to Ensure Desired Convergence.

Since the mechanism in Section 4 calls for the co-location of the sensor and observer, we plan to develop analogs where the transmissions between the output sensor and the observer are scheduled (where the observer is implemented remotely) and where exact knowledge of the observer values $\hat{x}(t)$ is not required.

Declaration of competing interest

The authors declare that they have no known competing financial interests or personal relationships that could have appeared to influence the work reported in this paper.

Appendix A. Checking Assumption 2

We provide two remarks on how to check Assumption 2.

Remark A.1. Assumption 2 can always be satisfied for a matrix $\Gamma > 0$ with small enough entries and a constant matrix K when (A, B) is a (constant) controllable pair, after a change of variables. This is done by choosing a constant matrix K such that all eigenvalues of $A+BK$ are negative real values, and then using a similarity transformation that transforms (A, B) into a new pair (PAP^{-1}, PB) where

$$H = P(A+BK)P^{-1} \tag{A.1}$$

is the (Hurwitz and Metzler) Jordan canonical form of $A+BK$. Then we can satisfy the requirements of Assumption 1 with a constant vector $V > 0$ (by [19, Lemma 2.3, p.41]). □

Remark A.2. Assumption 2 can also be satisfied in time-varying cases where $(A_0(t), B_0(t))$ has the form $(A_c + \Delta_A(t), B_c + \Delta_B(t))$ when (A_c, B_c) is a controllable pair and the sup norms of the continuous time-varying parts (Δ_A, Δ_B) and the entries of $\Gamma > 0$ are small enough, by applying the change of coordinates from Remark A.1 to (A_c, B_c). On the other hand, for any constant $\alpha > 0$, Assumption 2 is also satisfied by

$$\begin{aligned} &A_0(t) = 1 - \tfrac{\alpha\cos(\alpha t)}{2+\sin(\alpha t)},\ B_0 = 1,\ K = -4,\ \Gamma = \tfrac{c}{4}, \\ &V = 2+\sin(\alpha t),\ \overline{V} = 3,\ \underline{V} = 1,\ \text{and } p = 3-c \end{aligned} \tag{A.2}$$

for any constant $c \in (0, 3)$. This illustrates how Assumption 2 also allows cases where the supremum of A_0 can be arbitrarily large (because $\alpha > 0$ can be arbitrarily large). Then we can use numerical methods to find values $\nu > 0$ such that the requirements from Lemma B.1 hold. For instance, for $\alpha = 50$, they hold with (A.2), $c = 2.99$, and $\nu = 0.1$. □

Appendix B. Methods for choosing ν

A key ingredient in our theorem is the constant $\nu > 0$ satisfying our condition (7). The following lemma provides a sufficient condition for $\nu > 0$ to satisfy (7) (but see below for other ways to satisfy (7)):

Lemma B.1. *Let $\Gamma \in \mathbb{R}^{n\times n}$ be a positive matrix and Ω_0 be defined by (6). Fix constants $\bar{a} > 0$ and $\bar{b} > 0$ such that $\|A_0\|_\infty \le \bar{a}$ and $\|B_0K\|_\infty \le \bar{b}$. Let $\underline{\gamma} \in (0, \min\{1, r_0\})$ be a constant, where r_0 is the smallest of the entries of the matrix $\Gamma > 0$. Then for any constant $\nu > 0$ such that*

$$(1 + (\bar{b}/\bar{a}))(e^{\bar{a}\nu} - 1)e^{(1+(\bar{b}/\bar{a}))(e^{\bar{a}\nu}-1)} \le \underline{\gamma}, \tag{B.1}$$

our requirement (7) is satisfied. □

Proof. We show that $\Omega_0(t,s)$ is invertible and that

$$|I - \Omega_0^{-1}(t,s)| \le \Gamma \tag{B.2}$$

is satisfied when $t \in [s, s+\nu]$ and $s \ge 0$.

To prove the invertibility property, first note that since $\Phi_{A_0}(t,s)$ is invertible, it follows from the semigroup property of fundamental solutions that the matrix $\Omega_0(t,s)$ is invertible if and only if $\mathcal{N}(s,t) = I + \int_s^t \Phi_{A_0}(s,m)B_0(m)K(m)\mathrm{d}m$ is invertible. When $t \ge s$, this matrix is invertible if

$$\mathcal{L}(t,s) < 1, \tag{B.3}$$

where

$$\mathcal{L}(t,s) = \int_s^t \|\Phi_{A_0}(s,m)\|\|B_0(m)K(m)\|\mathrm{d}m \tag{B.4}$$

(by showing that the nullspace of $\mathcal{N}(s,t)$ is 0). Also,

$$\mathcal{L}(t,s) \le \int_s^t e^{\bar{a}(m-s)}\mathrm{d}m\bar{b} \le (\bar{b}/\bar{a})(e^{\bar{a}(t-s)} - 1) \tag{B.5}$$

when $t \ge s \ge 0$, e.g., by the Peano–Baker formula (e.g., from [21, Appendix C.4]). Since (B.1) implies that $(\bar{b}/\bar{a})(e^{\bar{a}\nu} - 1) < 1$, we deduce that the inequality (B.3) is satisfied for all $s \ge 0$ and $t \in [s, s+\nu]$, which implies that $\Omega_0(t,s)$ is invertible for all $s \ge 0$ and $t \in [s, s+\nu]$.

Next, we prove that (B.2) is satisfied for all $t \in [s, s+\nu]$, where $s \ge 0$ is arbitrary. Note that (B.2) is satisfied if

$$\left\|I - \Omega_0(t,s)^{-1}\right\| \le \underline{\gamma}. \tag{B.6}$$

This inequality is equivalent to

$$\left\|I - (I - \widetilde{\Omega}_0(t,s))^{-1}\right\| \le \underline{\gamma} \tag{B.7}$$

with $\widetilde{\Omega}_0(t,s) = I - \Omega_0(t,s)$. We prove that $\|\widetilde{\Omega}_0(t,s)\| < 1$ for all $t \in [s, s+\nu]$. Since

$$\begin{array}{l}\widetilde{\Omega}_0(t,s) = \\ I - \Phi_{A_0}(t,s) - \int_s^t \Phi_{A_0}(t,m)B_0(m)K(m)\mathrm{d}m,\end{array} \tag{B.8}$$

the inequality

$$\|\widetilde{\Omega}_0(t,s)\| \le \|I - \Phi_{A_0}(t,s)\| + (\bar{b}/\bar{a})(e^{\bar{a}(t-s)} - 1) \tag{B.9}$$

is satisfied when $t \ge s \ge 0$. The Peano–Baker formula gives

$$\left|\left|\Phi_{A_0}(t,s) - I\right|\right| \le \sum_{k=1}^{+\infty} \frac{(t-s)^k\|A_0\|_\infty^k}{k!} \le e^{\bar{a}(t-s)} - 1 \tag{B.10}$$

when $t \ge s \ge 0$. Thus (B.9) implies that

$$\begin{array}{rcl}\|\widetilde{\Omega}_0(t,s)\| & \le & e^{\bar{a}(t-s)} - 1 + (\bar{b}/\bar{a})(e^{\bar{a}(t-s)} - 1) \\ & = & (1 + (\bar{b}/\bar{a}))(e^{\bar{a}(t-s)} - 1)\end{array} \tag{B.11}$$

when $t \ge s \ge 0$. From (B.1), we deduce that $\|\widetilde{\Omega}_0(t,s)\| \le \underline{\gamma} < 1$ for all $t \in [s, s+\nu]$. Hence, by the matrix geometric series formula, the inequality (B.7) is equivalent to

$$\left\|\sum_{k=1}^{+\infty} \frac{\widetilde{\Omega}(t,s)^k}{k!}\right\| \le \underline{\gamma} \tag{B.12}$$

for all $t \in [s, s+\nu]$. It is satisfied if

$$\|\widetilde{\Omega}_0(t,s)\| \sum_{k=1}^{+\infty} \frac{\left\|\widetilde{\Omega}_0(t,s)\right\|^{k-1}}{(k-1)!} \le \underline{\gamma} \tag{B.13}$$

for all $t \in [s, s+\nu]$. This inequality is equivalent to

$$\|\widetilde{\Omega}_0(t,s)\|e^{\|\widetilde{\Omega}_0(t,s)\|} \le \underline{\gamma}. \tag{B.14}$$

According to (B.11), (B.14) is satisfied if

$$(1 + (\bar{b}/\bar{a}))(e^{\bar{a}(t-s)} - 1)e^{(1+(\bar{b}/\bar{a}))(e^{\bar{a}(t-s)}-1)} \le \underline{\gamma}. \tag{B.15}$$

By (B.1), this is the case. This concludes the proof. □

The optimal (i.e., largest) ν satisfying the requirements of Lemma B.1 is the ν such that (B.1) holds with equality, which is the root ν of

$$(1 + (\bar{b}/\bar{a}))(e^{\bar{a}\nu} - 1)e^{(1+(\bar{b}/\bar{a}))(e^{\bar{a}\nu}-1)} = \underline{\gamma}, \tag{B.16}$$

because the left side of (B.1) is strictly increasing in ν. We can use numerical methods to solve for the root $\nu > 0$ of (B.16). The constant ν constructed in the proof of Lemma B.1 is in general not the largest possible ν such that (7) is satisfied for given choices of A_0, B_0, K, and Γ. In practice, direct or numerical techniques can be applied to find values for ν that satisfy (7) but violate (B.1). To see how, we next consider other ways to satisfy (7), including a result for periodic cases which we used to compute ν in Remark A.2. See also Section 6.1 for an application to curve tracking.

First we consider the case where A_0, B_0, and K have the same period $p_* > 0$. Second, we consider a case where A_0 has the form $A_0(t) = A_c + \Delta_A(t)$ for a constant matrix A_c, where the known matrix-valued function Δ_A is bounded and continuous (but not necessarily periodic), under suitable bounds on the sup norm of Δ_A.

To cover the periodic case, first note that in this case, we have $\Phi_{A_0}(t,s) = \Phi_{A_0}(t - ip_*, s - ip_*)$ and so also $\Omega_0(t,s) = \Omega_0(t - ip_*, s - ip_*)$ for all integers $i \ge 0$, all $s \ge ip_*$ and all $t \ge s$, by our formula (6) for Ω_0. Hence, (7) will hold if $\nu > 0$ is such that (B.2) is satisfied for all $s \in [0, p_*]$ and $t \in [s, s+\nu]$. To see why, note that if (B.2) holds for all $s \in [0, p_*]$ and $t \in [s, s+\nu]$, and if $s_a \ge 0$ and $t_a \in [s_a, s_a+\nu]$ are given, then we can find an integer $i \ge 0$ such that $s_a \in [ip_*, (i+1)p_*]$, so

$$|I - \Omega_0^{-1}(t_a, s_a)| = |I - \Omega_0^{-1}(t_a - ip_*, s_a - ip_*)| \le \Gamma, \tag{B.17}$$

because $s_a - ip_* \in [0, p_*]$ and $t_a - ip_* \in [s_a - ip_*, s_a - ip_* + \nu]$. For any $\nu > 0$, we can use numerical methods to check whether (B.2) holds for all $s \in [0, p_*]$ and $t \in [s, s+\nu]$, because we can factor $\Phi_{A_0}(t,m)$ for all $m \in [s,t]$, $s \in [0, p_*]$, and $t \in [s, s+\nu]$, e.g., by writing

$$\Phi_{A_0}(t,m) = \alpha_A(t)\beta_A(m) \tag{B.18}$$

for all $m \ge 0$ and $t \ge m$, where α_A and β_A are the unique solutions of the matrix differential equations

$$\dot{\alpha}_A(t) = A_0(t)\alpha_A(t) \text{ and } \dot{\beta}_A(m) = -\beta_A(m)A_0(m) \tag{B.19}$$

that satisfy $\alpha_A(0) = \beta_A(0) = I$, and by then checking if

$$\sup\{|I - \Omega_0^{-1}(t,s)| : s \in [0, p_*], t \in [s, s+\nu]\} \le \Gamma; \tag{B.20}$$

see, e.g., [27], for the use of this decomposition of fundamental solutions in adaptive control. The factoring (B.18) makes it possible to compute the fundamental solution values that are needed to check Assumption 3.

To cover cases where $A_0(t) = A_c + \Delta_A(t)$ for a constant matrix A_c and continuous and bounded Δ_A, assume that the coefficient matrix $B = B_0$ is a known constant matrix, and that the requirements of Assumption 2 are satisfied for some $\Gamma > 0$ with a constant K, but similar reasoning applies if B and K are time varying.

Choose any positive matrices Γ_a and $\Gamma_b = [\gamma_{ij}]$ such that $\Gamma = \Gamma_a + \Gamma_b$. Then (7) is satisfied if $\nu > 0$ and Δ_A satisfy

$$\begin{array}{l}\sup_{\ell\in[0,\nu]} |I - \Omega_c^{-1}(\ell)| \leq \Gamma_a \text{ and} \\ \left\{b_* e^{\nu\|A_c\|}\left(e^{\nu\|\Delta_A\|_\infty} - 1\right)\right\}\|\Omega_c^{-1}\|_{[0,\nu]} < c_0,\end{array} \tag{B.21}$$

where $b_* = 1 + \nu\|BK\|$,

$$\Omega_c(s) = e^{sA_c} + \int_0^s e^{A_c(s-\ell)} \mathrm{d}\ell BK, \tag{B.22}$$

and the constant $c_0 \in (0, 1)$ is such that

$$\tfrac{c_0}{1-c_0}\|\Omega_c^{-1}\|_{[0,\nu]} \leq \min\left\{\gamma_{ij} : 1\leq i\leq n,\ 1\leq j\leq n\right\}. \tag{B.23}$$

To see why (7) is satisfied in this case, we first write

$$\begin{array}{rcl}\Omega_0(t,s) & = & \Omega_c(t-s) + \Phi_{A_0}(t,s) - e^{(t-s)A_c} \\ & & + \int_s^t \left[\Phi_{A_0}(t,\ell) - e^{A_c(t-\ell)}\right] BK\mathrm{d}\ell \\ & = & \Omega_c(t-s)\left[I + \eta(t,s)\right]\end{array} \tag{B.24}$$

for all $s \geq 0$ and $t \in [s, s+\nu]$, where

$$\begin{array}{l}\eta(t,s) = \Omega_c(t-s)^{-1}\big[\Phi_{A_0}(t,s) - e^{A_c(t-s)} \\ + \int_s^t \left(\Phi_{A_0}(t,\ell) - e^{A_c(t-\ell)}\right) BK\mathrm{d}\ell\big].\end{array} \tag{B.25}$$

Using the bound

$$\left\|\Phi_{A_0}(t,\ell) - e^{A_c(t-\ell)}\right\| \leq e^{\nu\|A_c\|}\left(e^{\nu\|\Delta_A\|_\infty} - 1\right) \tag{B.26}$$

which holds for all $\ell \in [s, t]$, $s \geq 0$, and $t \in [s, s+\nu]$, e.g., by [28, Lemma 2], and recalling (B.21), it follows that $\|\eta(t,s)\| \leq c_0 < 1$, and therefore that $I + \eta(t,s)$ is invertible (by checking that its nullspace is trivial). This implies that (B.24) is invertible when $s \geq 0$ and $t \in [s, s+\nu]$

Also, for $\bar{c} = \min_{ij}\gamma_{ij}$, and for any $S \in \mathbb{R}^{n\times n}$ that satisfies $\|S\| \leq \bar{c}$, we have $|S| \leq \Gamma_b$. Specializing the preceding observation to the case where $S = \Omega_c(t-s)^{-1} - \Omega_0^{-1}(t,s)$, it follows from Lemma C.1 in Appendix C (applied with $M_0 = \Omega_c(t-s)$, N_0 being the quantity in squared brackets in (B.25), $\bar{m} = \|\Omega_c^{-1}\|_{[0,\nu]}$, and $\bar{n}$ being the quantity in curly braces in (B.21)) that (B.23) gives

$$\begin{array}{l}\left\|M_0^{-1} - (M_0+N_0)^{-1}\right\| \\ = \left\|\Omega_c(t-s)^{-1} - \Omega_0^{-1}(t,s)\right\| \leq \frac{\|\Omega_c^{-1}\|_{[0,\nu]}c_0}{1-c_0} \\ \leq \min\{\gamma_{ij} : 1\leq i\leq n,\ 1\leq j\leq n\},\end{array} \tag{B.27}$$

and so also

$$\left|\Omega_c(t-s)^{-1} - \Omega_0^{-1}(t,s)\right| \leq \Gamma_b, \tag{B.28}$$

by writing $\Omega_0(t,s) = M_0 + N_0$ and then noting that $\|M_0^{-1}\|\|N_0\| \leq c_0$. Hence, the bound $|I - \Omega_0^{-1}(t,s)| \leq \Gamma$ for all $s \geq 0$ and $t \in [s, s+\nu]$ follows from the first inequality in (B.21) and (B.28) and our decomposition $\Gamma = \Gamma_a + \Gamma_b$. Conditions (B.21) can be checked numerically by computing Ω_c in (B.22), and they hold for a small enough $\nu > 0$ because $\Omega_c(0) = I$, by the continuity of matrix inversion.

Using the preceding alternative conditions (B.21) instead of (B.1) from Lemma B.1, we can allow cases with bigger values of ν, and therefore ensure less frequent recomputations of control values. For instance, consider the scalar case where $A_c = B_0 = 1$, $K = -2.2$, Δ_A is bounded by 0.1, $\Gamma = 0.35$, and $\nu = 0.16$. Then, simple Mathematica calculations show that condition (B.1) is violated, because with the choices $\bar{a} = 1.1$ and $\bar{b} = 2.2$, the left side of (B.1) is $1.02834 > \min\{1, \Gamma\} = 0.35$. On the other hand, the criteria (B.21) are satisfied with the preceding choices of A_c, B_0, K, Γ, and ν and any Δ_A that is bounded by 0.1, if we choose $c_0 = 0.0526$, $\Gamma_a = 0.79\Gamma$, and $\Gamma_b = 0.21\Gamma$.

Appendix C. Lemmas from [28]

We used the following lemmas (which are [28, Lemma 1], and a variant of [29, Lemma 1] with a similar proof, respectively) in Appendix B:

Lemma C.1. *Let $M_0 \in \mathbb{R}^{n\times n}$ be an invertible matrix. Let $N_0 \in \mathbb{R}^{n\times n}$ be a matrix. Let $\bar{n}$ and $\bar{m}$ be two constants such that $\|M_0^{-1}\| \leq \bar{m}$ and $\|N_0\| \leq \bar{n}$. Assume that $\bar{m}\bar{n} < 1$. Then the matrix $M_0 + N_0$ is invertible and*

$$\left\|M_0^{-1} - (M_0+N_0)^{-1}\right\| \leq \frac{\bar{m}^2\bar{n}}{1-\bar{m}\bar{n}} \tag{C.1}$$

is satisfied. □

Lemma C.2. *Consider the system*

$$\dot{\zeta}(t) = [\mathcal{A}(t) + \mathcal{E}(t)]\,\zeta(t) \tag{C.2}$$

where $\mathcal{A} : [0, +\infty) \to \mathbb{R}^{n\times n}$ is a continuous matrix-valued function, ζ is valued in $\mathbb{R}^n$, and $\mathcal{E} : [0, +\infty) \to \mathbb{R}^{n\times n}$ has piecewise continuous entries. Then for all $t_1 \in \mathbb{R}$ and $t_2 \in \mathbb{R}$ such that $t_1 \geq t_2$, the inequality

$$\begin{array}{l}\|\Phi_{\mathcal{A}+\mathcal{E}}(t_1,t_2) - \Phi_{\mathcal{A}}(t_1,t_2)\| \\ \leq e^{\|\mathcal{A}\|_\infty(t_1-t_2)}\left(e^{\|\mathcal{E}\|_\infty(t_1-t_2)} - 1\right)\end{array} \tag{C.3}$$

is satisfied. □

References

[1] F. Brunner, W.P.M.H. Heemels, F. Allgower, Event-triggered and self-triggered control for linear systems based on reachable sets, Automatica 101 (2019) 15–26.

[2] T. Henningsson, E. Johannesson, A. Cervin, Sporadic event-based control of first-order linear stochastic systems, Automatica 44 (11) (2008) 2890–2895.

[3] W. Heemels, K. Johansson, P. Tabuada, An introduction to event-triggered and self-triggered control, in: Proceedings of 51st IEEE conference on decision and control, Maui, Hawaii, 2012, pp. 3270–3285.

[4] J. Peralez, V. Andrieu, M. Nadri, U. Serres, Event-triggered output feedback stabilization via dynamic high-gain scaling, IEEE Trans. Automat. Control 63 (8) (2018) 2537–2549.

[5] A. Selivanov, E. Fridman, Distributed event-triggered control of transport-reaction systems, IFAC-PapersOnLine 48 (11) (2015) 593–597.

[6] A. Selivanov, E. Fridman, Event-triggered H_∞ control: A switching approach, IEEE Trans. Automat. Control 61 (10) (2016) 3221–3226.

[7] A. Selivanov, E. Fridman, Event-triggered adaptive control of minimum-phase systems, IFAC-PapersOnLine 50 (1) (2017) 4276–4281.

[8] P. Tabuada, Event-triggered real-time scheduling of stabilizing control tasks, IEEE Trans. Automat. Control 52 (9) (2007) 1680–1685.

[9] X. Wang, M. Lemmon, Self-triggered feedback control systems with finite-gain L_2 stability, IEEE Trans. Automat. Control 54 (3) (2009) 452–467.

[10] Z.-P. Jiang, T. Liu, Small-gain theory for stability and control of dynamical networks: A survey, Annu. Rev. Control 46 (2018) 58–79.

[11] T. Liu, Z.-P. Jiang, A small-gain approach to robust event-triggered control of nonlinear systems, IEEE Trans. Automat. Control 60 (8) (2015) 2072–2085.

[12] W. Heemels, J. Sandee, P. van den Bosch, Analysis of event-driven controllers for linear systems, Internat. J. Control 81 (2008) 571–590.

[13] J. Yook, D. Tilbury, N. Soparkar, Trading computation for bandwidth: Reducing communication in distributed control systems using state estimators, IEEE Trans. Control Syst. Technol. 10 (4) (2002) 503–518.

[14] J.-L. Gouzé, A. Rapaport, Z. Hadj-Sadok, Interval observers for uncertain biological systems, Ecol. Model. 133 (1–2) (2000) 45–56.

[15] F. Mazenc, O. Bernard, Interval observers for linear time-invariant systems with disturbances, Automatica 47 (1) (2011) 140–147.

[16] T. Raissi, D. Efimov, A. Zolghadri, Interval state estimation for a class of nonlinear systems, IEEE Trans. Automat. Control 57 (1) (2012) 260–265.

[17] F. Mazenc, M. Malisoff, Stability analysis for time-varying systems with delay using linear Lyapunov functionals and a positive systems approach, IEEE Trans. Automat. Control 61 (3) (2016) 771–776.

[18] E. Fornasini, M. Valcher, Linear copositive Lyapunov functions for continuous-time positive switched systems, IEEE Trans. Automat. Control 55 (8) (2010) 1933–1937.
[19] W. Haddad, V. Chellaboina, Q. Hui, Nonnegative and Compartmental Dynamical Systems, Princeton University Press, Princeton, NJ, 2010.
[20] F. Mazenc, M. Malisoff, C. Barbalata, Z.-P. Jiang, Event-triggered control using a positive systems approach, European J. Control 62 (2021) 63–68, Special Issue on the European Control Conference.
[21] E. Sontag, Mathematical Control Theory, second ed., Springer, New York, NY, 1998.
[22] F. Mazenc, V. Andrieu, M. Malisoff, Design of continuous-discrete observers for time-varying nonlinear systems, Automatica 57 (7) (2015) 135–144.
[23] T. Liu, P. Zhang, Z.-P. Jiang, Robust Event-Triggered Control of Nonlinear Systems, Springer, Singapore, 2020.
[24] M. Malisoff, F. Zhang, Adaptive control for planar curve tracking under controller uncertainty, Automatica 49 (5) (2013) 1411–1418.
[25] F. Zhang, E. Justh, P. Krishnaprasad, Boundary following using gyroscopic control, in: Proceedings of the IEEE conference on decision and control. Nassau, Bahamas, 2004, pp. 5204-5209.
[26] M. Malisoff, F. Zhang, Robustness of adaptive control under time delays for three-dimensional curve tracking, SIAM J. Control Optim. 53 (4) (2015) 2203–2236.
[27] M. Malisoff, Tracking and parameter identification for model reference adaptive control, Internat. J. Robust Nonlinear Control 30 (4) (2020) 1582–1606.
[28] F. Mazenc, S. Ahmed, M. Malisoff, Finite time estimation through a continuous-discrete observer, Internat. J. Robust Nonlinear Control 28 (16) (2018) 4831–4849.
[29] F. Mazenc, S. Ahmed, M. Malisoff, Reduced order finite time observers and output feedback for time-varying nonlinear systems, Automatica 119 (2020) 109083.